

A Novel Wideband Dual-Band Dual-Polarized Magneto-Electric Dipole Antenna

Fan Li, Yufa Sun*, Haoran Zhu, Junnan Yu, and Yade Fang

Abstract—In this paper, a novel wideband dual-band dual-polarized magneto-electric (ME) dipole antenna is proposed. The proposed antenna consists of a folded double-layer magneto-electric dipole, a stair-shaped feeding line with a balun structure and a rectangular box-shaped reflector. The folded double-layer magneto-electric dipole is able to generate two resonant frequencies. The polygon balun structure can better match the antenna impedance. The rectangular box-shaped reflector not only can suppress antenna's back radiation but also can realize high gain over the operating frequencies. Both simulated and measured results show that the antenna can obtain two wide impedance bandwidths of 60% (1.54–2.87 GHz) in lower frequency band and 27% (4.62–6.10 GHz) in higher frequency band with the reflection coefficients lower than 10 dB for both input ports. The isolation between ports is greater than 25 dB in the corresponding frequency band. The gains of the measured antenna were 8.5–9.7 dBi in the low frequency band and 8.5–11.5 dBi in the high frequency band, respectively.

1. INTRODUCTION

With the accelerating developments of wireless communications, the types of mobile services and number of communications users continue to increase exponentially. The society demands higher quality and speed of communications. The wideband or multiband antennas are needed to satisfy the increasing number of service bands, especially the WLAN, WiMAX, LTE and 5G (4.8–5 GHz) operating frequency bands. Compared to a traditional single band antenna, a multiband antenna can effectively decrease the number of antenna elements and covering areas [1]. Over the last few years, dual-polarized antennas have been widely used in base stations because they can provide polarization diversity to reduce side effects of multipath fading and can also increase channel capacity [2]. Meanwhile, wideband dual-band, high isolation and low cross-polarization electrical characteristics with a compact size are the huge problems for the wideband dual-band dual-polarized antenna.

In recent years, several dual-polarized antennas with good performances were designed based on slot antennas [3, 4] and dipole antennas [5, 6]. Several studies have been focused on the development of dual-band antenna elements [7–16]. To realize multiple bands, the most general method in the patch antenna is to etch various slots on the radiation patch or ground plane. In [7, 8], the proposed antennas obtain multiple bands by etching slots on monopole antennas. In the magneto-electric (ME) antenna, two common methods are proposed usually to achieve dual-band. The first method is to use dual-frequency band antenna elements to realize this feature concurrently. For instance, one antenna integrates lower and higher frequency band elements and then realizes dual-band dual-polarized electric characteristics ranging from 1.68 to 2.84 GHz and 5.31 to 5.95 GHz in [9]. The other one is to put interleaved single frequency band antenna elements together to obtain dual-band dual-polarized characteristics. As presented in [10], a dual-frequency dual-polarized antenna with roughly 6 dBi gain is composed of two

Received 3 August 2018, Accepted 25 September 2018, Scheduled 7 October 2018

* Corresponding author: Yufa Sun (yfsun_ahu@sina.com).

The authors are with the Key Lab of Intelligent Computing & Signal Processing, Ministry of Education, Anhui University, Hefei 230601, China.

different elements for different bands. A few dual-band dual-polarized antennas are proposed in [16, 17], and they exhibit good performance over the whole working bands, while its impedance bandwidth is not broad.

In this paper, a wideband dual-band dual-polarized magneto-electric antenna is presented. A folded metal double-layer magneto-electric dipole is deployed to generate the dual resonant frequencies. The dual-band dual-polarized antenna is the first one used by folded metal double-layer, and polygon baluns are used in middle of stair-shaped feeding strips to improve match impedance. Moreover, owing to the rectangular box-shaped reflector, the antenna's back radiation can be suppressed, and high gain can be achieved across the operating frequency range. Besides, due to the special feeding structure, the proposed antenna exhibits better performance in impedance bandwidth, and it can also obtain two wide impedance bandwidths of 60% (1.54–2.87 GHz) in low frequency band and 27% (4.62–6.10 GHz) in high frequency band with the reflection coefficients lower than 10 dB for both input ports. Moreover, it is more suitable for 2G/3G/LTE/5G(4.8–5 GHz)/WiMAX/WLAN application.

This paper is organized as follows. In Section 2, the basic structure and operation principle of the proposed antenna are described. The detailed design process of the proposed antenna and experiment results of the antenna are given in Section 3. Parameter study is discussed in Section 4. The comparison of different dual-band antennas is discussed in Section 5, followed by the conclusions which are presented in Section 6.

2. ANTENNA DESCRIPTIONS

2.1. Antenna Structure

The geometry of the dual-band dual-polarized magneto-electric dipole is shown in Figs. 1–2. Two resonant frequency points of a low frequency and a high frequency are excited by the folded double-layer metal patch. For dual polarizations, two linearly polarized magneto-electric dipole elements are located orthogonally. As shown in Fig. 1, the proposed antenna consists of a rectangular reflector, two pairs of orthogonal folded double-layer metal patches and a pair of orthogonal stair-shaped feeding strips. At the middle of the feeding strips, a polygonal balun structure is used to match the impedance. A rectangular reflector is used to achieve stable gain and better radiation in the passband.

As shown in Fig. 2, stair-shaped feeding strips are used to excite the antenna. In fact, the feeding strip has two functions: one is a coupled strip, and the other is a transmission strip. The coupling strip is stair-shaped which can be considered as the combination of two L -shaped strips with different lengths. Indeed, the stair-shaped feeding strip achieves more degree of freedom for impedance tuning than other feeding structures. Its horizontal part is responsible for coupling electrical energy to antenna. The vertical part incorporated with one of the vertical patches introduces some capacitance to compensate the inductance caused by the horizontal part. The trapezoid line is used for the transmission portion to increase the impedance bandwidth which is narrower at the top (W_4 and W_7 at each polarization) and wider at the bottom (W_3 and W_6 at each polarization). SMA connector located under the ground plane is connected to the bottom of the stair-shaped strip line.

For dual polarizations, two stair-shaped feeding strips are placed orthogonally at different heights to avoid mechanical interference. With the help of High Frequency Structure Simulator (HFSS) software, the dimensions of the configurations are simulated and optimized, and the final optimal dimension values are listed in Table 1.

In fabrication of the prototype, the proposed antenna is made of brass, and the thickness of brass patch is 1 mm. The radius of the two SMA probes is 0.6 mm, and they protrude by 5 mm above the box-shaped ground plane.

2.2. Principle of Operation

In our design, as shown in Fig. 1, the antenna is a combination of four pairs of horizontal plane dipoles (electric dipoles) and four pairs of vertically oriented folded shorted patches antennas (magnetic dipoles). The high band is excited by the bottom layer, and the low band is excited by the high layer. Therefore, dual-band operation is realized by the two-layer magneto-electric dipole.

Table 1. Dimensions for the proposed dual-band dual-polarized Magneto-electric antenna.

Parameters	L_g	L_1	L_2	L_3	L_4	W_1	W_2	W_3
Values/mm	110	6	26	18	5	12.5	24	4
Parameters	W_4	W_5	W_6	W_7	W_8	H_1	H_2	H_3
Values/mm	2.4	9	4.5	1.6	12	26.1	13	41.1
Parameters	H_4	H_5	H_6	H_7	H_g	d_1	d_2	d_3
Values/mm	10.4	18.5	15.6	15.5	25	0.8	1.2	1.3

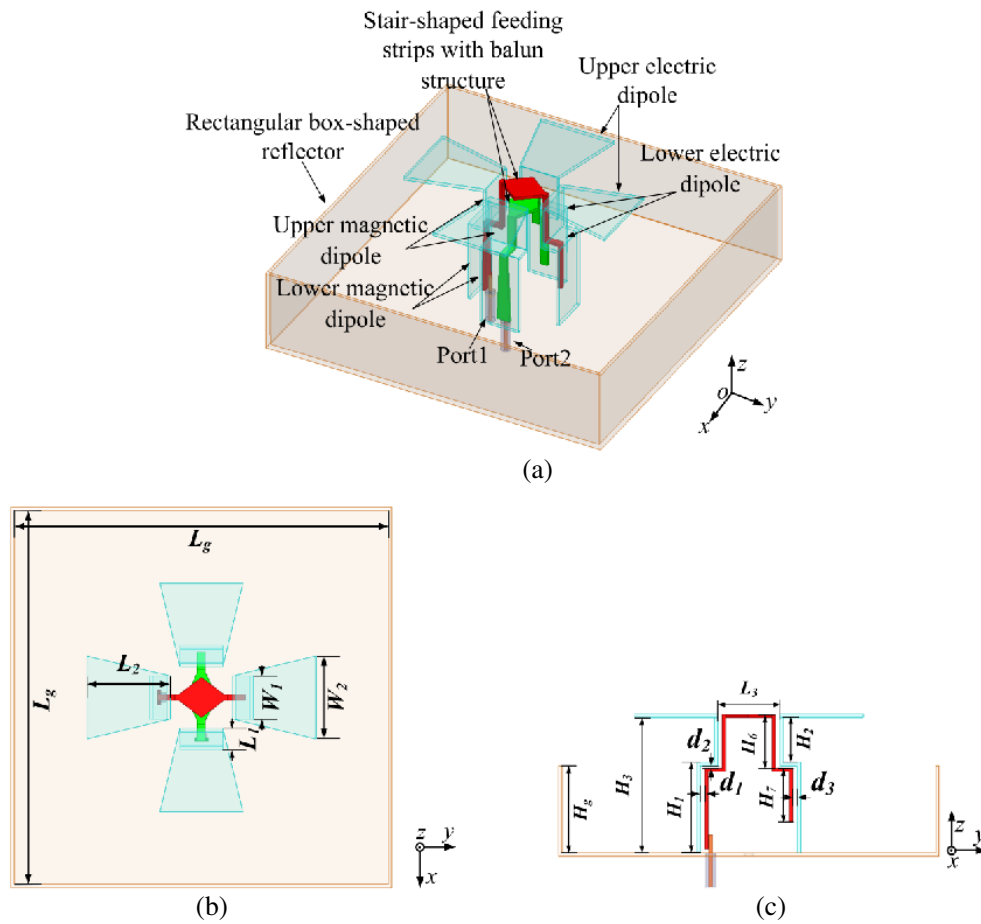


Figure 1. Perspective, top and side views of the dual-band dual-polarized antenna. (a) Perspective view. (b) Top view. (c) Side view.

To better understand the working principle of the antenna, the current distributions of the proposed antenna with input from port 1 and port 2, at time t_1 and t_2 are analyzed as shown in Fig. 3, respectively. Definition T is the period of the variation of the electromagnetic fields caused by the proposed antenna. At time $t_1 = t_2 = 0$, the currents are mainly distributed on the planar dipoles, whereas the currents on vertically oriented shorted patches are minimized. Therefore, it is clear that the electric dipole mode is mainly excited in the horizontal and vertical directions when port 1 and port 2 are excited at time $t_1 = t_2 = 0$, respectively. At time $t_1 = t_2 = T/4$, the currents distributed on the planar dipoles are minimized, whereas the currents on vertically oriented shorted patches are strongest, suggesting that the magnetic dipole mode is mainly excited in the horizontal and vertical directions when port 1 and

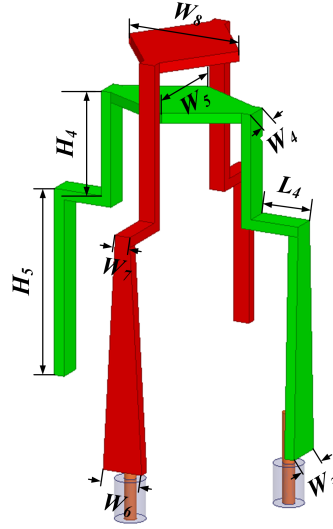


Figure 2. Geometry of the orthogonal stair-shaped feeding line with balun structure.

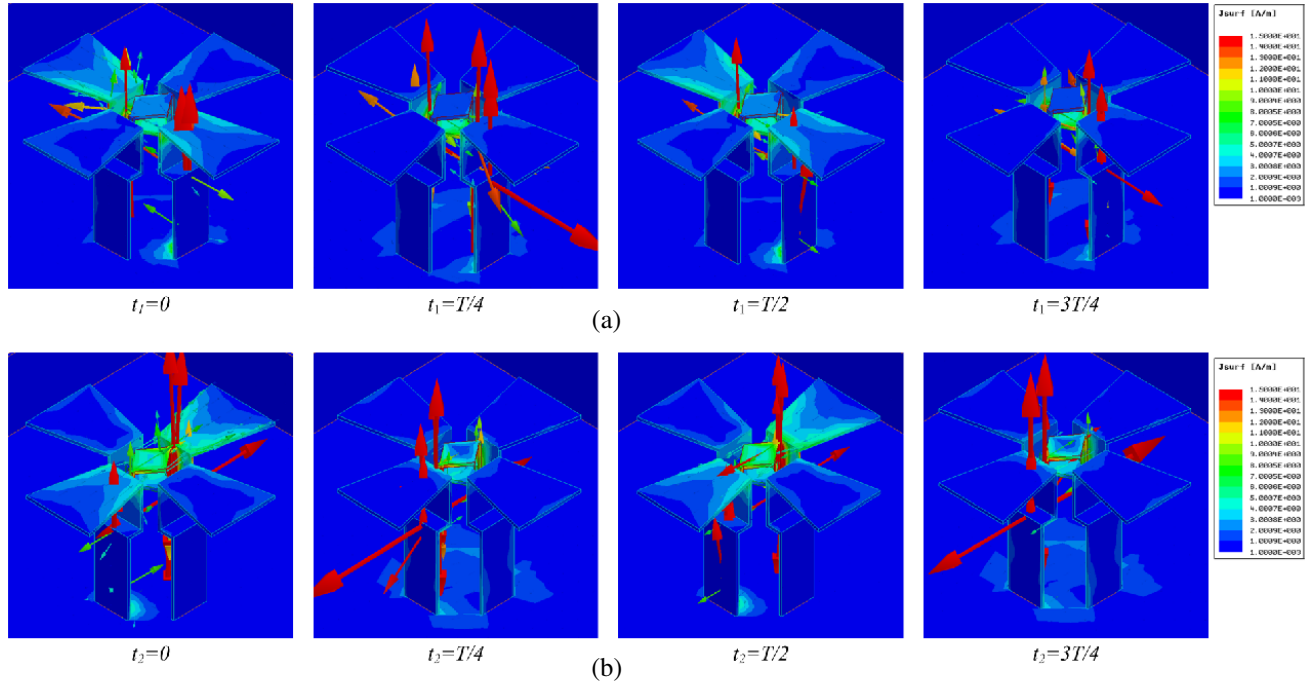


Figure 3. Current distributions of the dual-band dual-polarized antenna at 2.2 GHz. (a) Port 1; (b) Port 2.

port 2 are excited at time $t_1 = t_2 = T/4$, respectively. At time $t_1 = t_2 = T/2$, the electric dipole mode is mainly excited again with opposite current direction to the mode at $t_1 = t_2 = 0$. At time $t_1 = t_2 = 3T/4$, the magnetic dipole mode is mainly excited again with opposite current direction to the mode at $t_1 = t_2 = T/4$.

Hence, two degenerate modes of similar magnitude in strength are excited on the planar dipole (electric dipole) and the quarter-wave vertically oriented shorted patch antennas (magnetic dipole). The equivalent electric and magnetic currents are 90 degrees in phase difference and orthogonal to each other. It is expected that the antenna in this proposed form can achieve stable gain and low back radiation over the operating frequency band.

3. ANTENNA PERFORMANCE

3.1. Analysis of Antenna Design

In order to explain the antenna design process, Fig. 4 shows three structures. Ant. 1 is a single-band dual-polarized ME antenna. Ant. 2 folds the magnetic dipole on the basis of Ant. 1 to form a double-layer structure, thereby introducing a high-frequency resonance point. Ant. 3 is based on Ant. 2 to add polygonal baluns structure to the stair-shaped feeding line to adjust the impedance matching of low and high frequency bands. All antennas were analyzed using the finite element method of ANSYS HFSS. The S -parameters and gains of the three antennas are compared in Fig. 5. In Fig. 5(a), we can see that Ant. 1 has a resonant frequency range of 1.5 to 2.8 GHz in the low frequency band. The gain of Ant. 1 is shown in Fig. 5(d). However, from the simulation results we can see that Ant. 1 only has a low frequency band, so we propose Ant. 2, and the folded structure in antenna Ant. 2 introduces a high-frequency resonance point. Ant. 3 incorporates polygonal baluns structure in the middle of two feeders to better match the low and high frequency bands of Port 1 and Port 2, and to achieve the working requirements of low and high frequency bands.

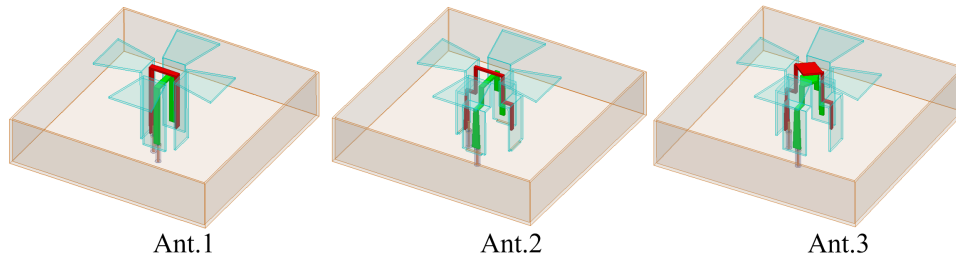


Figure 4. Three configurations in the evolution of the proposed antenna: Ant. 1: single-band dual-polarized antenna, Ant. 2: dual-band dual-polarized antenna and Ant. 3: dual-band dual-polarized with polygonal baluns antenna.

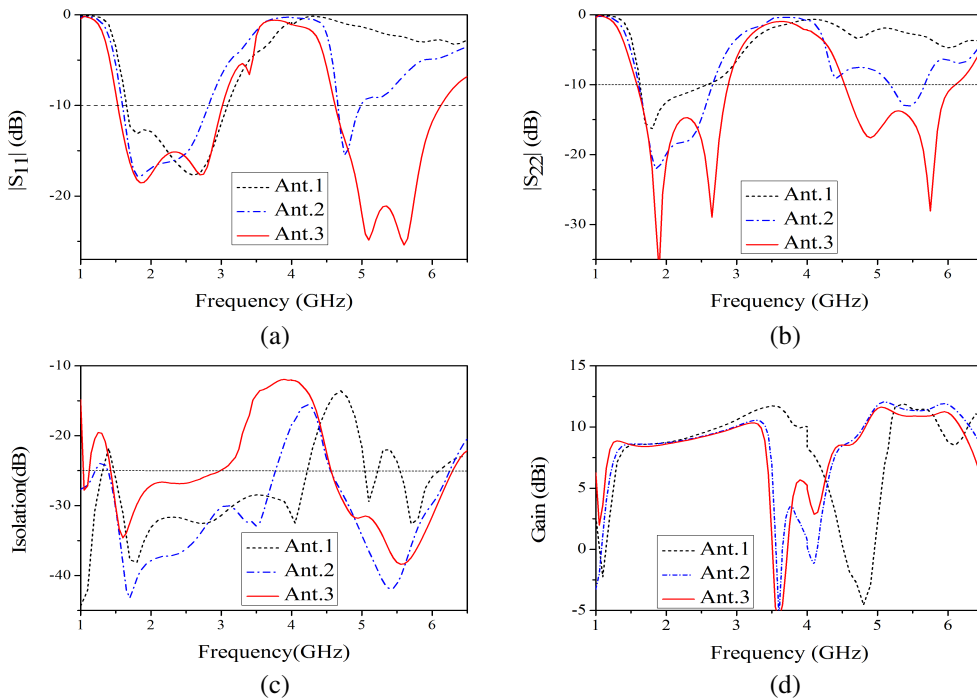


Figure 5. Comparison of three different antennas: (a) S_{11} . (b) S_{22} . (c) Isolation and (d) Gain.

3.2. Simulated and Measured Results

To verify the proposed design, an antenna prototype was constructed, as shown in Fig. 6. Measured results of S-parameters, gains, isolation and radiation patterns were obtained by Agilent N5247A network analyzer and a SATIMO antenna measurement system.

Figure 7 depicts simulated and measured S -parameters and gains of the proposed dual-band dual-polarized antenna. It can be seen that the antenna operates from 1.54 to 2.87 GHz with a bandwidth of 60% ($S_{11} < -10$ dB & $S_{22} < -10$ dB) and from 4.62 to 6.10 GHz with a bandwidth of 27% ($S_{11} < -10$ dB & $S_{22} < -10$ dB) for low frequency band and high frequency band, respectively. The operating frequency ranges for the two ports are slightly different due to the unequal heights and dimensions of the two orthogonal strip lines. The common bandwidths of the two ports are 60% ranging from 1.54 to 2.87 GHz at lower-band and 27% ranging from 4.62 to 6.10 GHz. Fig. 7(c) shows the isolation between the two ports. The measured isolation between the two ports is better than 25 dB over the entire operating frequency band. Over the operating frequency range, the measured broadside gains for lower band and higher band are 9.1 ± 0.6 dBi and 10 ± 1.5 dBi, respectively.

The measured radiation patterns of the proposed dual-band dual-polarized magneto-electric dipole antenna for port 1 and port 2 at frequencies 2.2, 2.7, 5.5 and 5.8 GHz are plotted in Fig. 8. It is shown that the antenna has a nearly symmetric and good unidirectional radiation pattern across the entire bandwidth.

Detailed measured results including the Half-Power beamwidth in both horizontal and vertical planes, and the Cross-Polarization Level at two ports are summarized in Table 2. The Half-Power beamwidth in both horizontal and vertical planes for both ports becomes narrower as frequency increases. The cross-polarization levels for both H - and V -planes are less than -18 dB.

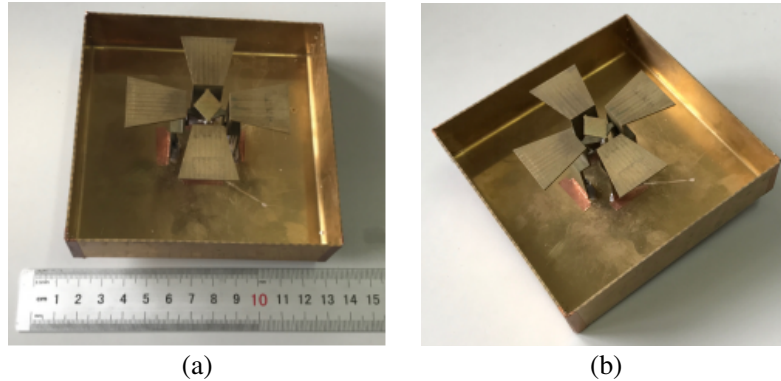


Figure 6. Prototype of the dual-band dual-polarized antenna: (a) top view of Ant. 3, and (b) perspective view of Ant. 3.

Table 2. Half-power beamwidth and cross-polarization level.

Frequency (GHz)	Port 1		Port 2		Cross-Polarization Level (dB)
	Half-Power beamwidth		Half-Power beamwidth		
	H -plane	V -plane	H -plane	V -plane	
2.2	61.7°	78.2°	77.7°	62.2°	-22
2.7	61.7°	78.2°	67.1°	56.1°	-18
5.0	28.6°	23.9°	24.1°	30.6°	-20
5.8	28.9°	26.3°	21.2°	30.5°	-25

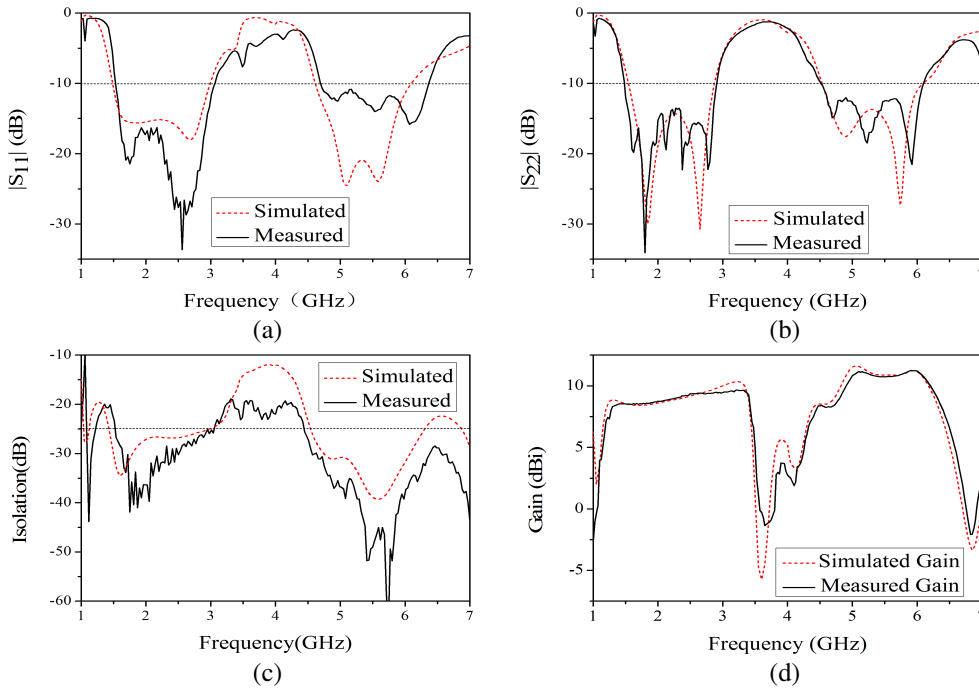


Figure 7. Simulated and measured: (a) S_{11} . (b) S_{22} . (c) Isolation and (d) Gain.

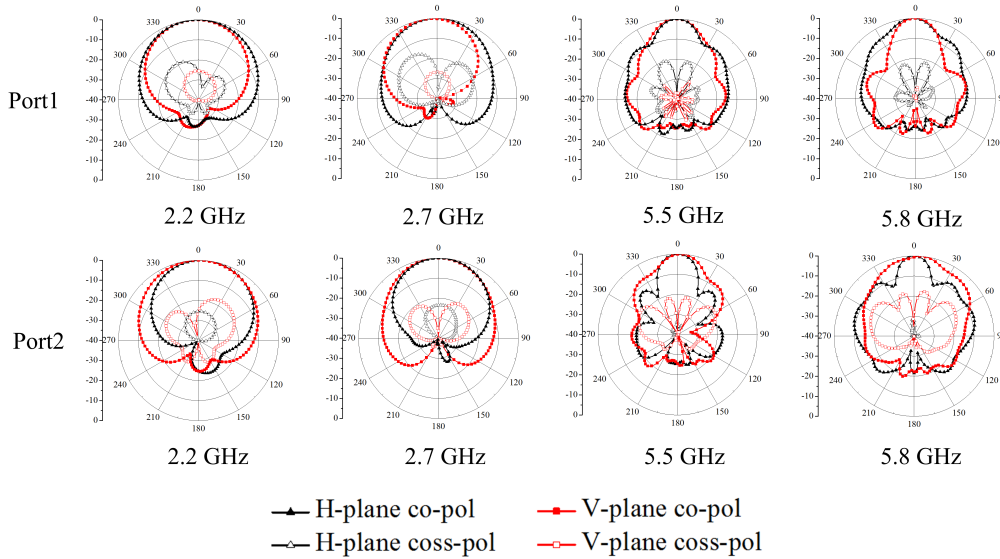


Figure 8. Measured radiation patterns of the dual-polarized antenna at frequencies of 2.2, 2.7, 5.5 and 5.8 GHz.

4. PARAMETRIC STUDY

4.1. Effects of Polygonal Balun

As we all know, the feeding strip in port 1 has a great influence on S_{11} and has a weak influence on S_{22} . The feeding strip in port 2 has a great influence on S_{22} and has a weak influence on S_{11} . Therefore, we only analyze the effect of width W_5 of the polygonal balun structure in port 1 on S_{11} . The effect on S_{22} is analyzed for width W_8 of the polygonal balun structure in port 2.

As shown in Figs. 9(a), (b), W_5 plays an important role in matching the high frequency band of the proposed antenna S_{11} , and W_8 also plays a crucial role in matching the high frequency band of the proposed antenna S_{22} . With the increase of W_5 and W_8 , the high-frequency matching of the antenna gradually becomes better, but it cannot be increased all the time, and the problem of isolation between two ports must be considered. Taken together, the choice of $W_5 = 9$ mm and $W_8 = 12$ mm is most suitable. Therefore, it is considered that the polygonal balun structure in the feeding line has an irreplaceable role in the proposed dual-frequency dual-polarized antenna.

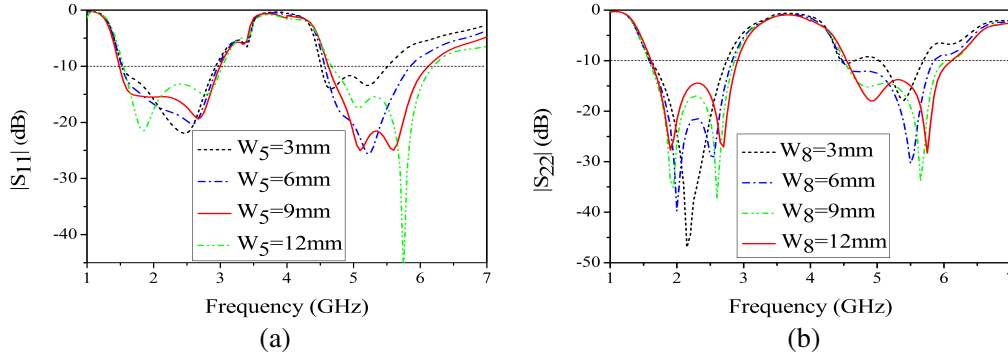


Figure 9. Effects of Polygonal Balun: (a) Effects of W_5 on S_{11} and (b) effects of W_8 on S_{22} .

4.2. Effect of Folded Double-Layer ME Dipole

The first and the most important parameter is the length L_2 of the horizontal portion of the planar dipole. It can be observed from Fig. 10 that S -parameters are highly sensitive to the value of L_2 . If L_2 is increased so that the electric dipole is enlarged, the resonance position of the low frequency band shifts to a lower frequency position. The lower electric dipole, due to the covering effect of the upper electric dipole, makes the bandwidth and the suppression depth of the high frequency band smaller. Therefore, to achieve a good impedance matching and stable gain over a wide frequency band, $L_2 = 26$ mm is selected.

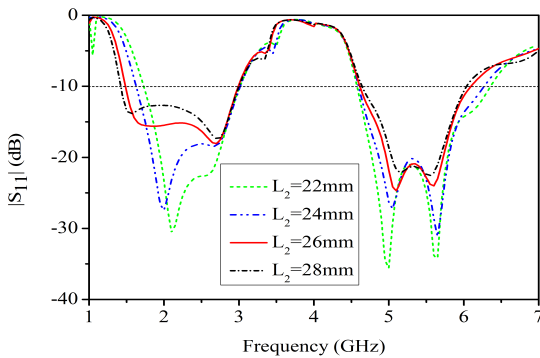


Figure 10. Effects of L_2 on S_{11} .

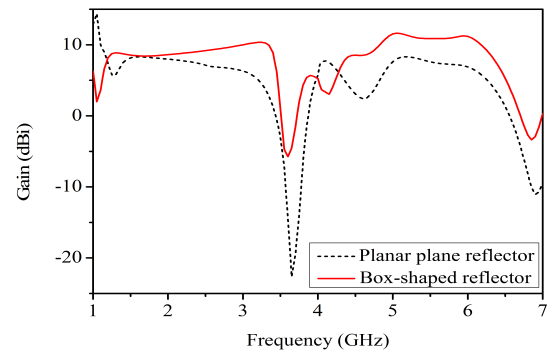


Figure 11. Effects of the reflectors on gain.

4.3. Effects of the Reflectors

To achieve high gain, a rectangular box-shaped reflector is necessary for a unidirectional antenna. To understand the usefulness of such a reflector, the antenna with a rectangular box-shaped reflector and a planar reflector was analyzed. As shown in Fig. 11, with a rectangular box-shaped reflector, the gain is much higher than the other. Fig. 12 depicts the simulated radiation patterns when port 1 is excited

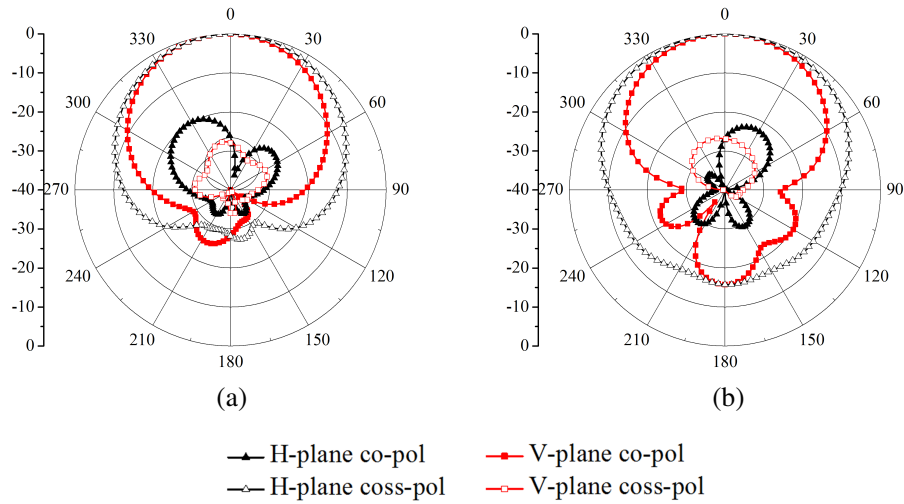


Figure 12. Simulated radiation patterns of the dual-band dual-polarized antenna. (a) With rectangular box-shaped reflector at 2.2 GHz; (b) With planar reflector at 2.2 GHz.

at 2.2 GHz for the dual-band dual-polarized antenna using the rectangular box-shaped reflector and the planar reflector. It can be seen that back radiation was suppressed by the box-shaped reflector. In other words, the rectangular box-shaped reflector is conducive to improving the antenna performances.

5. COMPARISON

The measured characteristics of the proposed antenna are compared with previous works in Table 3. The size of the antenna is related to the wavelength at the center frequency of the low frequency band. In the dual-polarized dual-band antennas listed in Table 3, the proposed antenna is wider than the reference antennas in the low-frequency and high-frequency bands. We can find that the proposed antenna in this paper has dual frequencies, dual polarizations and wide impedance bandwidth.

Table 3. Comparison of proposed antenna and references.

Ref.	Lower Band (GHz)	Upper Band (GHz)	Polarization	Size (λ_L)
[9]	1.68–2.84 (51.3%)	5.31–5.95 (11.4%)	Single	$1.05 \times 1.05 \times 0.286$
[11]	1.48–3.15 (72%)	4.67–5.78 (21%)	Single	$0.926 \times 0.926 \times 0.185$
[14]	0.78–1.1 (34%)	1.58–2.62 (49.5)	Single	$0.689 \times 0.689 \times 0.179$
[16]	0.8–0.96 (18%)	1.7–2.7 (45%)	Dual	$0.611 \times 0.611 \times 0.151$
[17]	2.4–2.48 (3.3%)	5.15–5.85 (12.7%)	Dual	$0.813 \times 0.813 \times 0.244$
This Work	1.54–2.87 (60%)	4.62–6.1 (27%)	Dual	$0.808 \times 0.808 \times 0.316$

λ_L is the wavelength at the center frequency of the lower working band.

6. CONCLUSION

A novel dual-band dual-polarized magneto-electric antenna is proposed. The proposed antenna exhibits better performance in impedance bandwidth, and it can obtain two wide impedance bandwidths of 60% (1.54–2.87 GHz) in lower frequency band and 27% (4.62–6.10 GHz) in higher frequency band with the reflection coefficients lower than 10 dB for both input ports. In addition, it is more suitable for 2G/3G/LTE/5G (4.8–5 GHz)/WiMAX/WLAN application.

ACKNOWLEDGMENT

This work is supported by the National Natural Science Foundation of China under Grant 61172020 and the Key Natural Science Project of Anhui Provincial Education Department (KJ2018A0020).

REFERENCES

1. Shuai, C.-Y. and G.-M. Wang, "A novel planar printed dual-band magneto-electric dipole antenna," *IEEE Access*, Vol. 5, 10062–10067, 2017.
2. Guo, Y.-X., K.-M. Luk, and K.-F. Lee, "Broadband dual-polarization patch element for cellular-phone base stations," *IEEE Trans. Antennas Propag.*, Vol. 50, No. 2, 251–253, 2002.
3. Li, B., et al., "Wideband dual-polarized patch antenna with low cross polarization and high isolation," *IEEE Antennas Wireless Propag. Lett.*, Vol. 11, 417–430, 2012.
4. Paryani, R. C., P. F. Wahid, and N. Behdad, "A wideband, dual-polarized, substrate-integrated cavity-backed slot antenna," *IEEE Antennas Wireless Propag. Lett.*, Vol. 9, 645–648, 2010.
5. Zhou, S.-G., P.-K. Tan, and T.-H. Chio, "Low-profile, wideband dual-Polarized antenna with high isolation and low cross polarization," *IEEE Antennas Wireless Propag. Lett.*, Vol. 11, 1032–1035, 2012.
6. Cui, Y. H., R. L. Li, and P. Wang, "A novel broadband planar antenna for 2G/3G/LTE base stations," *IEEE Trans. Antennas Propag.*, Vol. 61, No. 5, 2767–2774, 2013.
7. Wang, K. L. and L. C. Lee, "Multiband printed monopole slot antenna for WWAN operation in the laptop computer," *IEEE Trans. Antennas Propag.*, Vol. 57, No. 4, 324–330, Feb. 2009.
8. Xu, Y., Y.-C. Jiao, and Y.-C. Luan, "Compact CWP-fed printed monopole antenna with triple-band characteristics for WLAN/WiMAX applications," *Electron. Lett.*, Vol. 48, No. 24, 1519–1520, Nov. 2012.
9. Feng, B., W. An, S. Yin, et al., "Dual-wideband complementary antenna with a dual-layer cross-ME-dipole structure for 2G/3G/LTE/WLAN applications," *IEEE Antennas Wireless Propag. Lett.*, Vol. 14, 626–629, 2015.
10. Huang, T. J. and H. T. Hsu, "A dual-frequency and dual-polarization antenna design for long term evolution applications," *2015 IEEE International Symposium on Antennas and Propagation & USNC/URSI National Radio Science Meeting*, IEEE, 2009–2010.
11. He, K., S.-X. Gong, and F. Gao, "A wideband dual-band magneto-electric dipole antenna with improved feeding structure," *IEEE Antennas Wireless Propag. Lett.*, Vol. 13, 1729–1732, 2014.
12. Feng, B., et al., "A dual-wideband double-layer magnetoelectric dipole antenna with a modified horned reflector for 2G/3G/LTE applications," *International Journal of Antennas and Propagation*, Vol. 2013, 2013.
13. Feng, B., Q. Zeng, and M. Wang, "Substrate integrated magneto-electric dipole antenna for WLAN and WiMAX applications," *2016 IEEE MTT-S International Conference on Numerical Electromagnetic and Multiphysics Modeling and Optimization (NEMO)*, IEEE, 2016.
14. An, W. X., et al., "Design of broadband dual-band dipole for base station antenna," *IEEE Trans. Antennas Propag.*, Vol. 60, No. 3, 1592–1595, 2012.
15. Tao, J. and Q. Feng, "Dual-band magneto-electric dipole antenna with dual-sense circularly polarized character," *IEEE Trans. Antennas Propag.*, Vol. 65, No. 11, 5677–5685, 2017.
16. Yang, L., et al., "A dual-wideband dual-polarized directional magneto-electric dipole antenna," *Microwave and Optical Technology Letters*, Vol. 59, No. 5, 1128–1133, 2017.
17. Row, J.-S. and Y.-J. Huang, "Dual-band dual-polarized antenna for WLAN applications," *Microwave and Optical Technology Letters*, Vol. 60, No. 1, 260–265, 2018.